Electronic Supplementary Material (ESI) for Journal of Materials Chemistry A.

SUPPLEMENTARY DATA

Size Effects and Hydrogen Storage Properties of Mg Nanoparticles Synthesised by Electroless Reduction Method

Wei Liu, Kondo-Francois Aguey-Zinsou*

MERLin group, School of Chemical Engineering, The University of New South Wales, Sydney, NSW 2052, Australia

*Corresponding author: Tel.: +61 (0)2 938 57970; Fax: +61 (0)2 938 55966;
E-mail address: f.aguey@unsw.edu.au

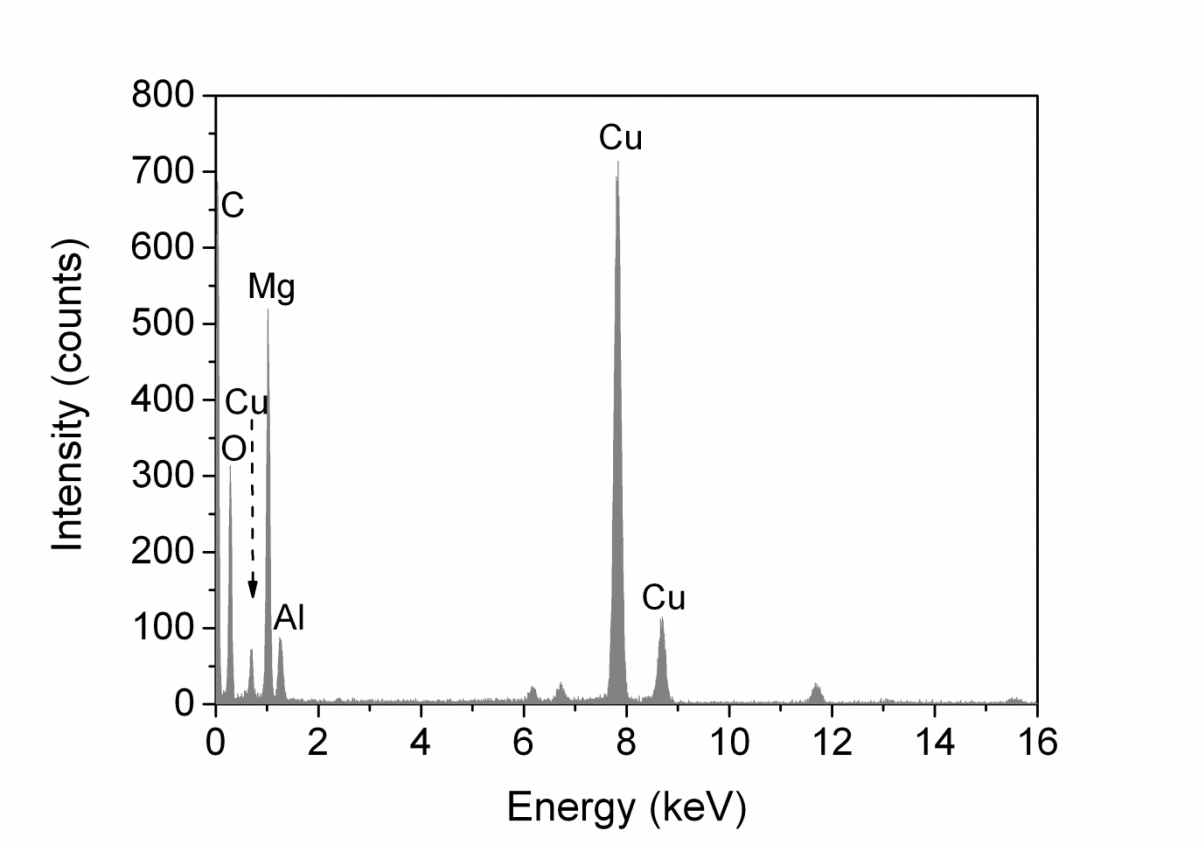

Fig. S1. Typical EDS analysis of the as-synthesised Mg nanoparticles observed by TEM

Aluminium is from triethylaluminum which acts as a viscosity reducer in di-*n*-butylmagnesium.

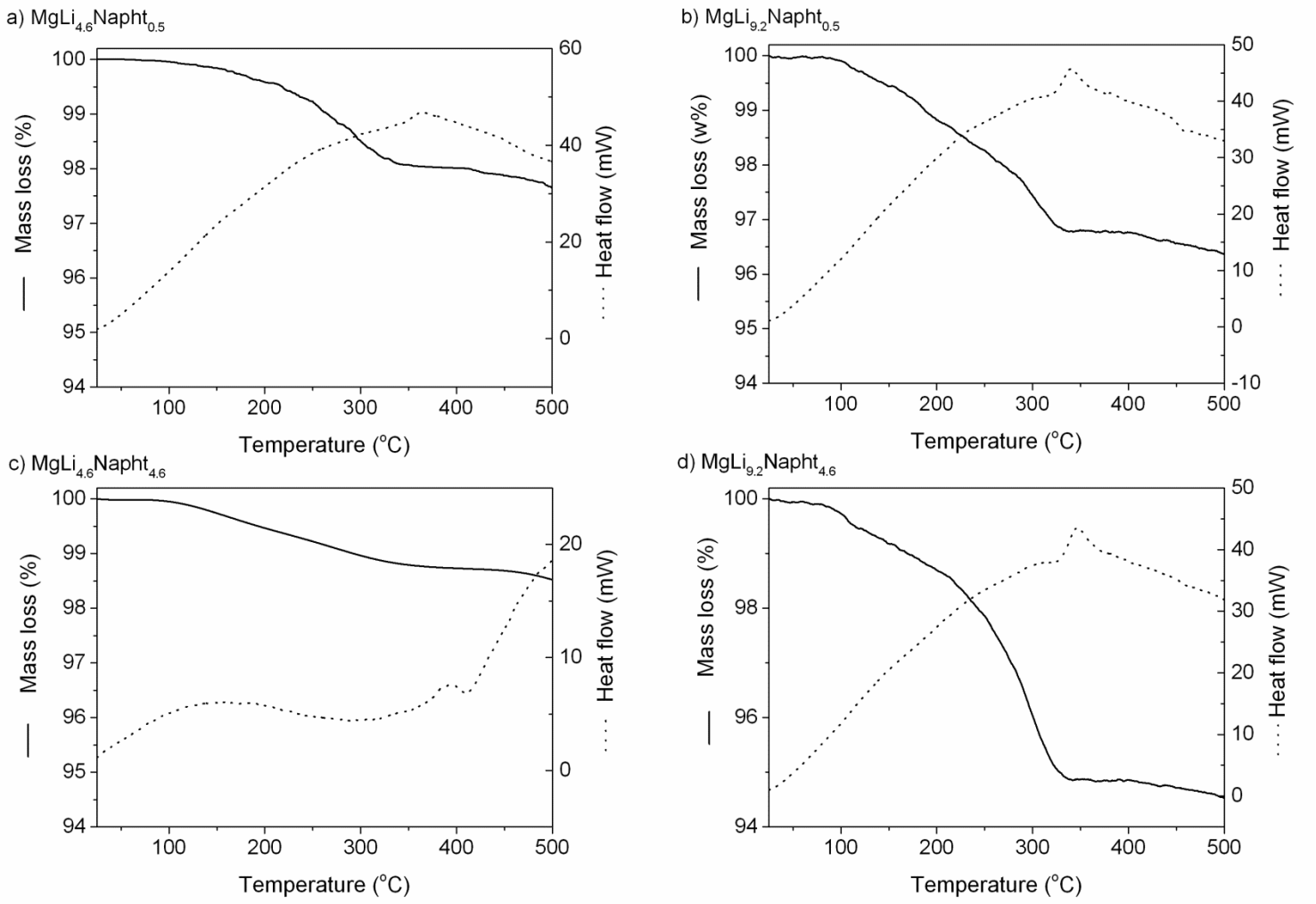

Fig. S2. TGA/DSC curves of the as-synthesised materials.

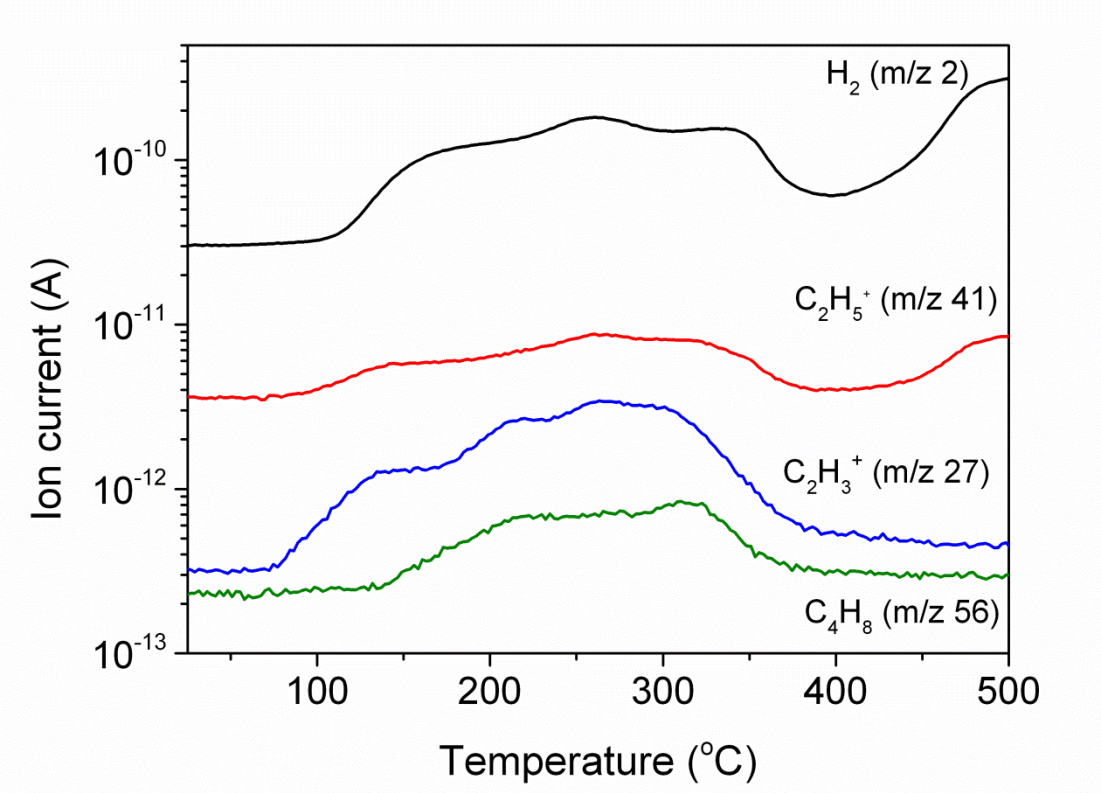

Fig. S3. Typical MS for the as-synthesised materials. Case of $MgLi_{4.6}Napth_{0.5}$.

The decomposition of *n*-butyllithium occurs following the reaction (1) below with the release of butane as detected by MS.

$$CH_3CH_2CH_2CH_2Li \rightarrow LiH + CH_3CH_2CH{=}CH_2 \quad (1)$$

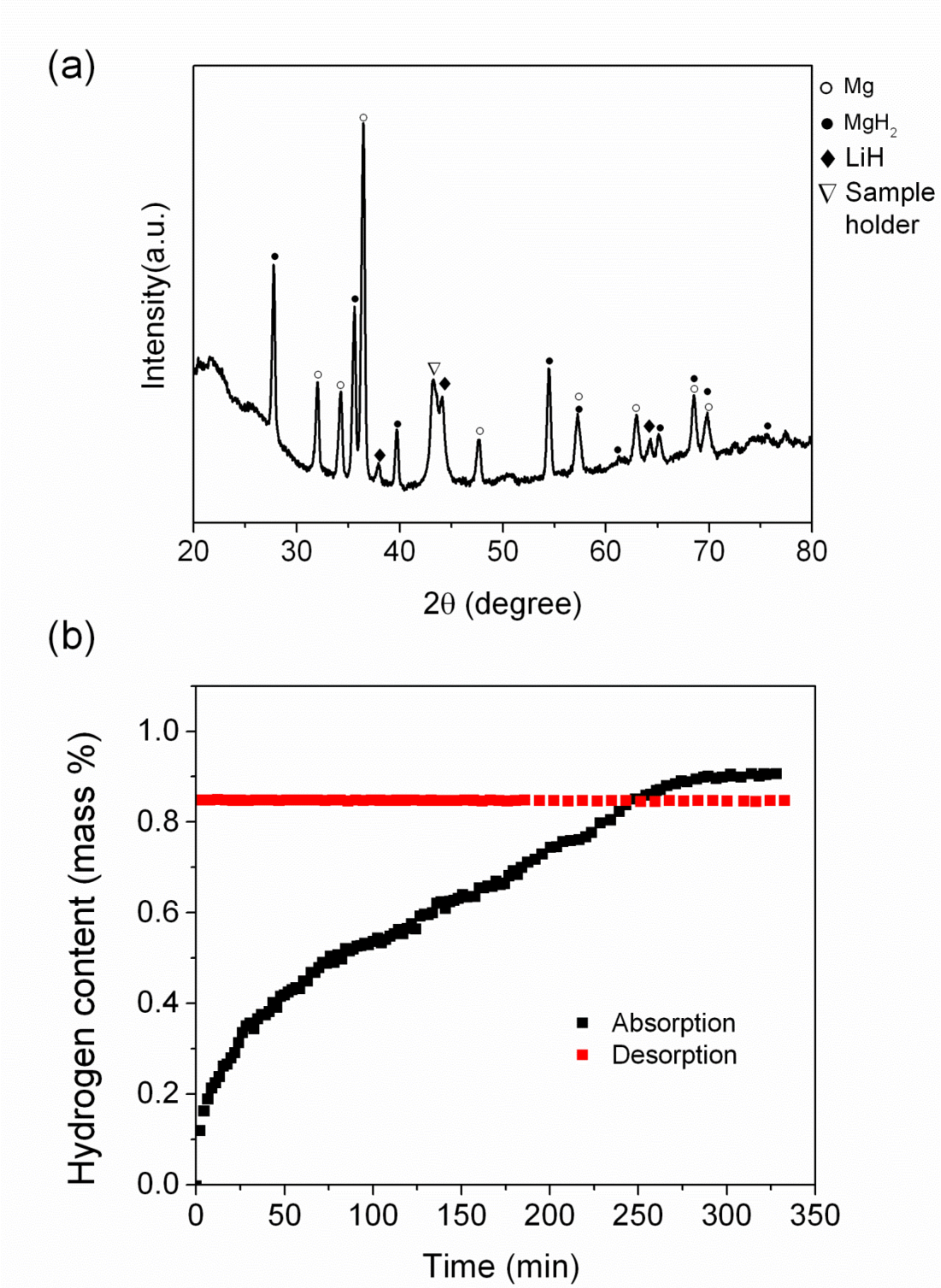

Fig. S4: a) XRD profile of $MgLi_{9.2}Napht_{0.5}$ hydrogenated at 120 °C under 30 bar hydrogen pressure, and b) associated hydrogen sorption kinetics.

The material could absorb hydrogen at 120 °C only. However, no desorption was achieved at this temperature under a pressure of 10 kPa.

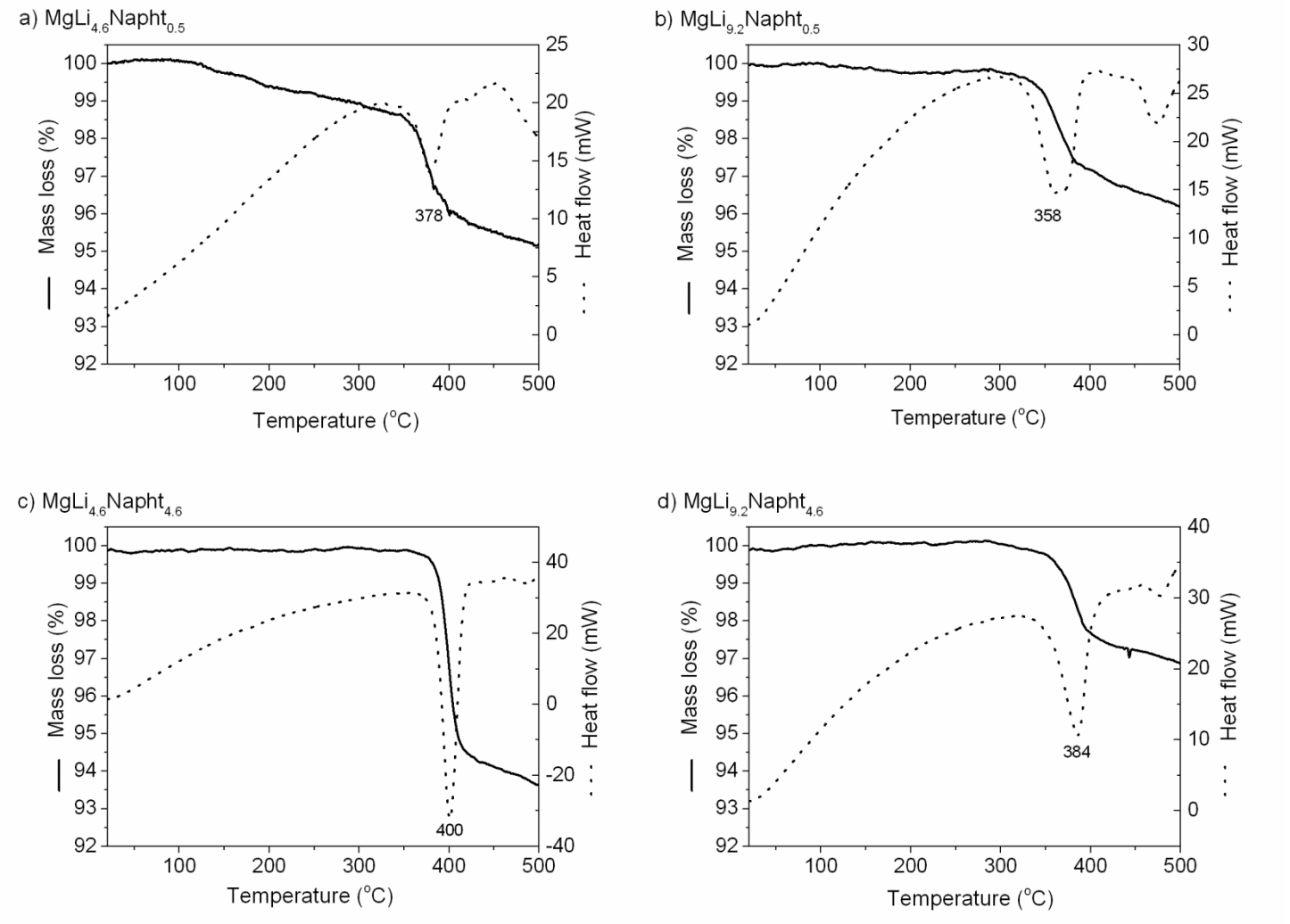

Fig. S5: TGA/DSC of the materials after hydrogen absorption at 300 °C.

The mass loss observed correspond to the decomposition of the β-MgH_2 into Mg with hydrogen release. This event is correlated with a strong endothermic peak with a maximum varying from 358 to 384 °C depending on the material. At higher temperatures (> 450 °C), the additional endothermic peak correspond to the decomposition of LiH into Li as proven by the release of hydrogen recorder by MS (Fig. 5).

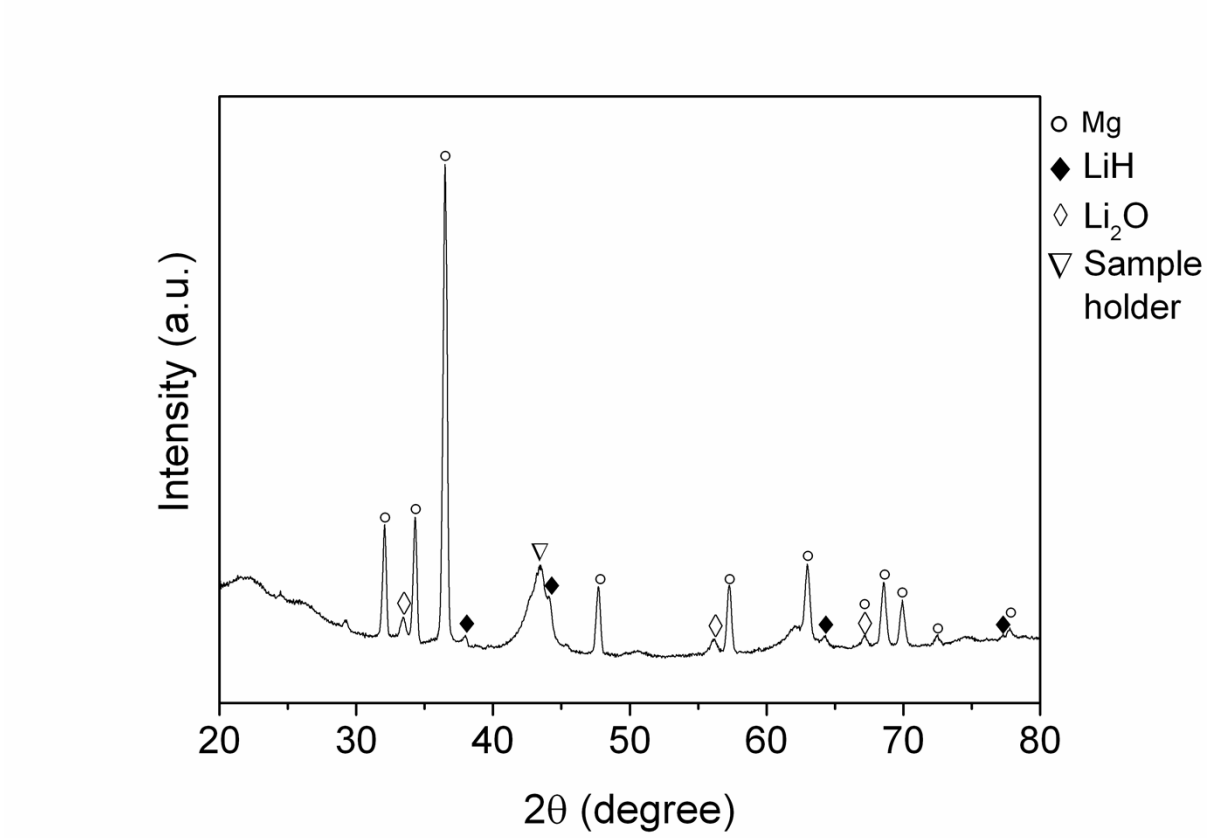

Fig. S6: Typical XRD pattern of the materials after hydrogen desorption at 300 °C.

The LiH phase does not decompose at 300 °C in agreement with TGA/MS measurements. The Li_2O may be due to a partial oxidation of the material during the XRD measurement.

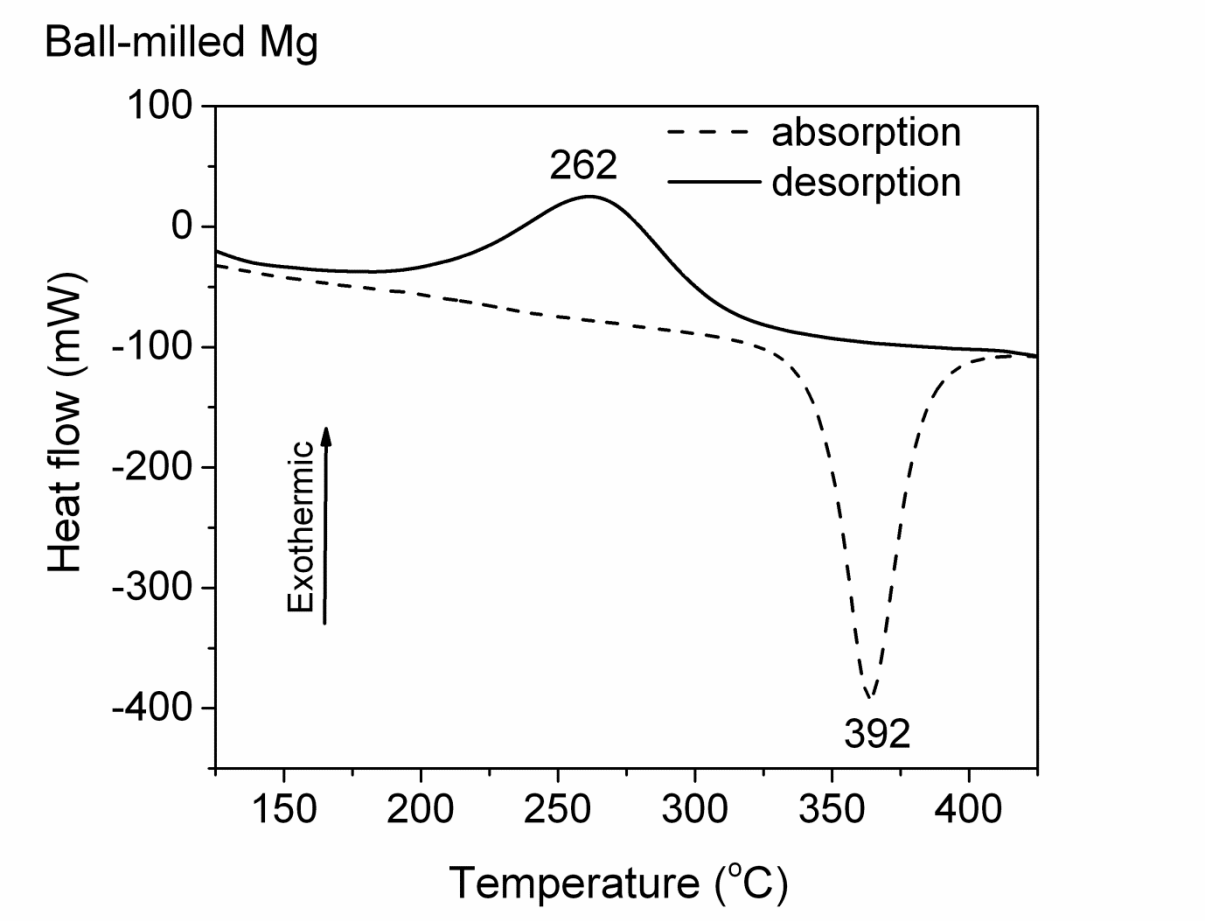

Fig. S7: HP-DSC curves for hydrogen absorption and desorption with ball milled MgH_2.

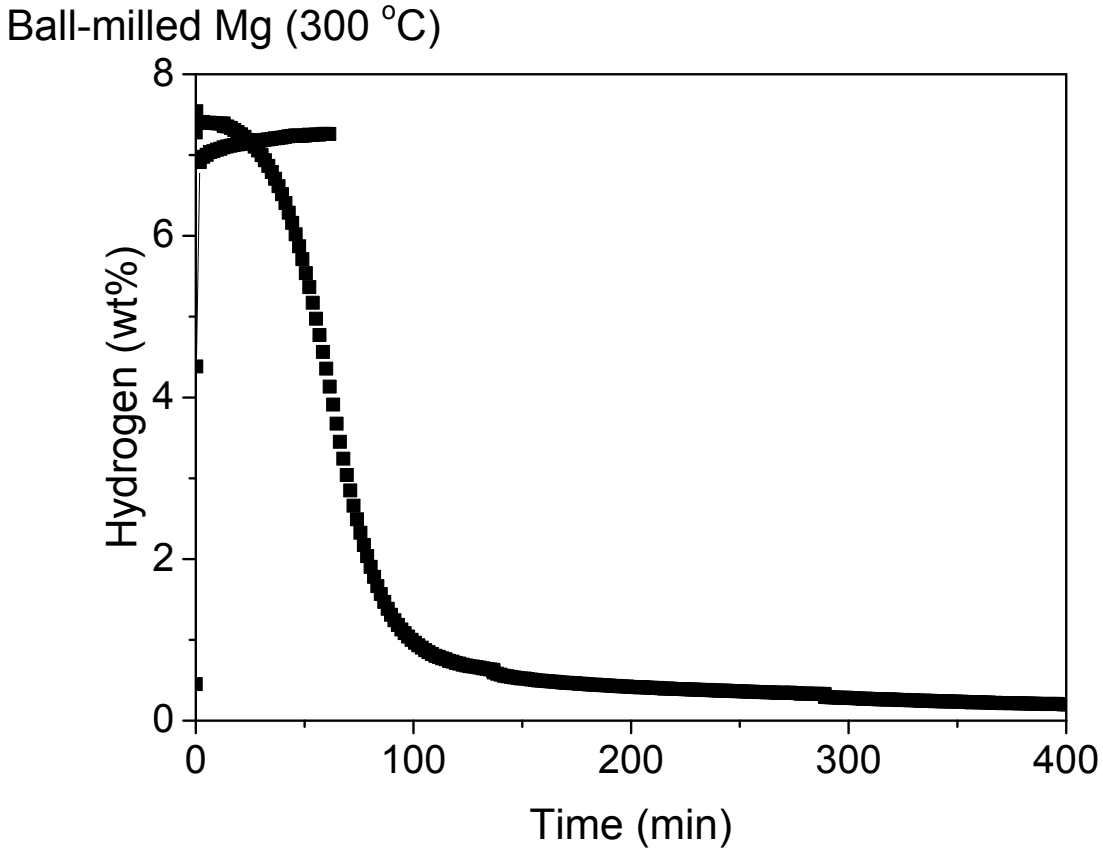

Fig. S8: Kinetic curves for hydrogen absorption and desorption with ball-milled MgH_2.

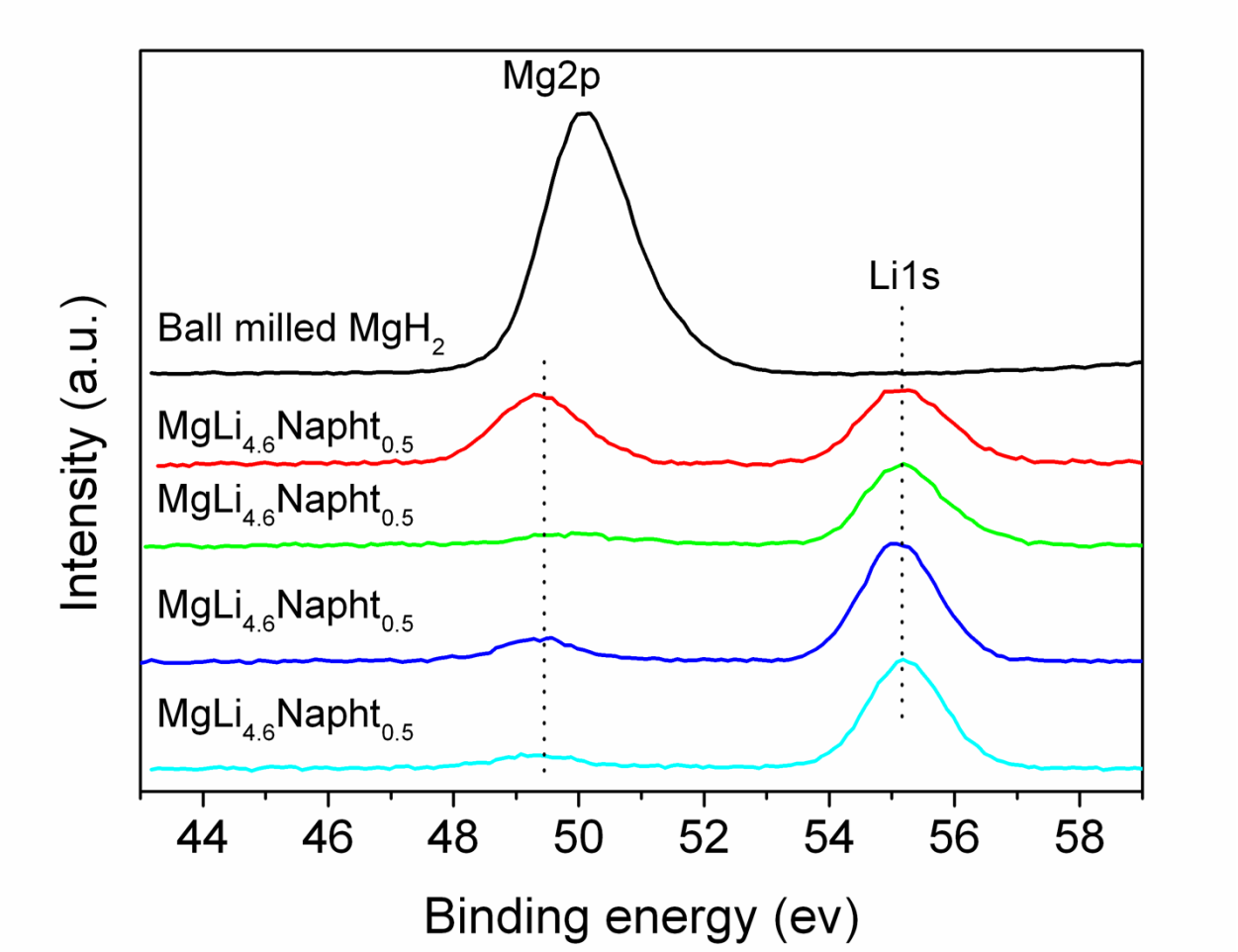

Fig. S9: XPS narrow-scan of Mg2p and Li1s for ball-milled MgH_2 and the Mg nanoparticles synthesised after hydrogen cycling.

Table S1: Elemental surface composition (atomic percentage, %) as determined by XPS for ball-milled MgH_2 and the Mg nanoparticles synthesised after hydrogen cycling.

	Binding energy (eV)			Surface composition (at%)			
	Li1s	Mg1s	Mg2p	Li1s	Mg2p	C1s	O1s
Ball milled MgH_2	-	1304.0	50.1, 51.4	-	46.85	8.86	34.13
$MgLi_{4.6}Napht_{0.5}$	55.2	1303.5	49.4	31.21	5.04	19.58	44.17
$MgLi_{9.2}Napht_{0.5}$	55.2	1303.6	49.6	34.75	0.95	19.47	44.83
$MgLi_{4.6}Napht_{4.6}$	55.1	1303.4	49.3	36.17	1.14	17.18	45.50
$MgLi_{9.2}Napht_{4.6}$	55.2	-	49.2	35.97	0.77	18.83	43.80

XPS analysis of ball-milled MgH_2 displays a Mg2p peak at 51.4 eV attributed to the formation MgO or $Mg(OH)_x$, and a Mg2p peak at 50.1 eV and Mg1s peak at 1304 eV attributed to metallic magnesium (Table s1).[1] In addition to the Mg1s peak corresponding to magnesium metallic, the nanoparticles synthesised and cycled display only one Mg2p peak also corresponding to metallic magnesium (Table S1).

XPS analysis also reveals a Li1s peak at 55.2 eV for the nanoparticles synthesised and cycled (Fig. S12). This peak can be attributed to Li_2CO_3 and may result from a partial surface contamination of the materials with CO_2 upon transfer in air to the XPS instrument.[2]

Additional determination of surface composition showed than the surface nanoparticles synthesised was mainly composed of Li, Mg, O and C. The O and C content of the surface may be due to a partial oxidation/contamination of the surface upon transfer of the materials in air to the instrument and the thickness of this surface oxide/contamination may have influenced the detection of metallic magnesium.

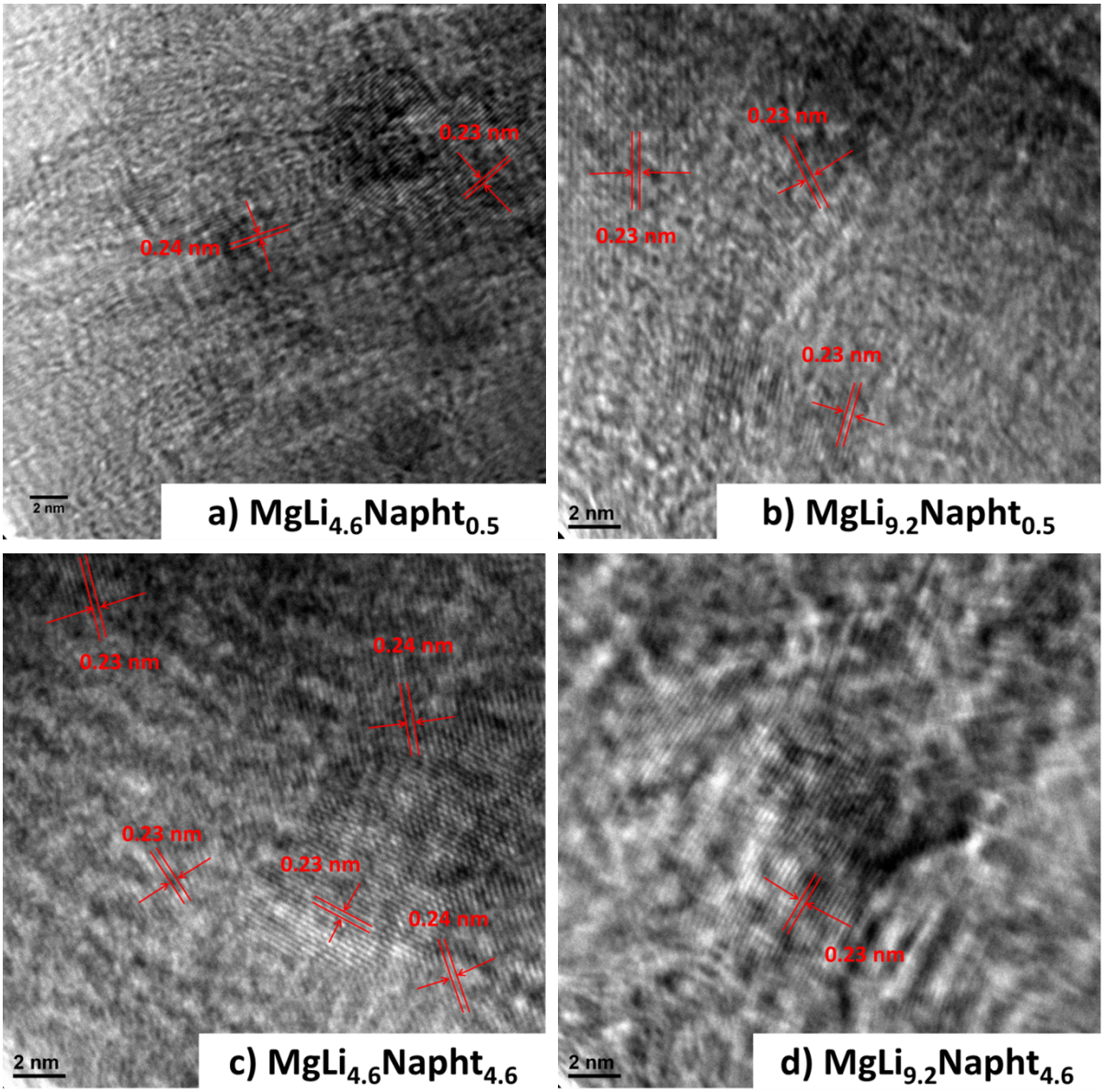

Fig. S10: HRTEM of the Mg nanoparticles after cycling.

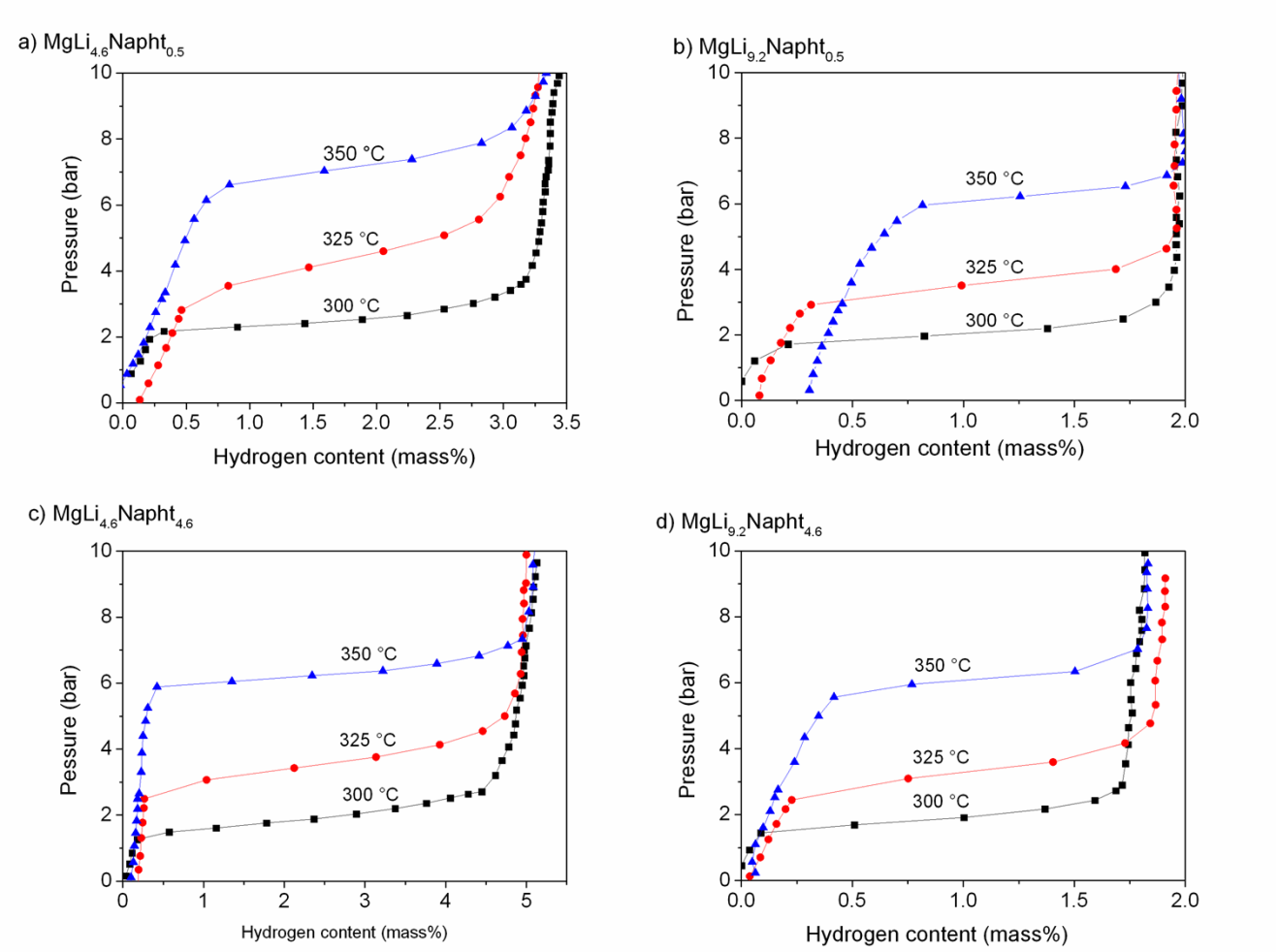

Fig. S11: PCI corresponding to the absorption of hydrogen within the Mg nanoparticles synthesised.

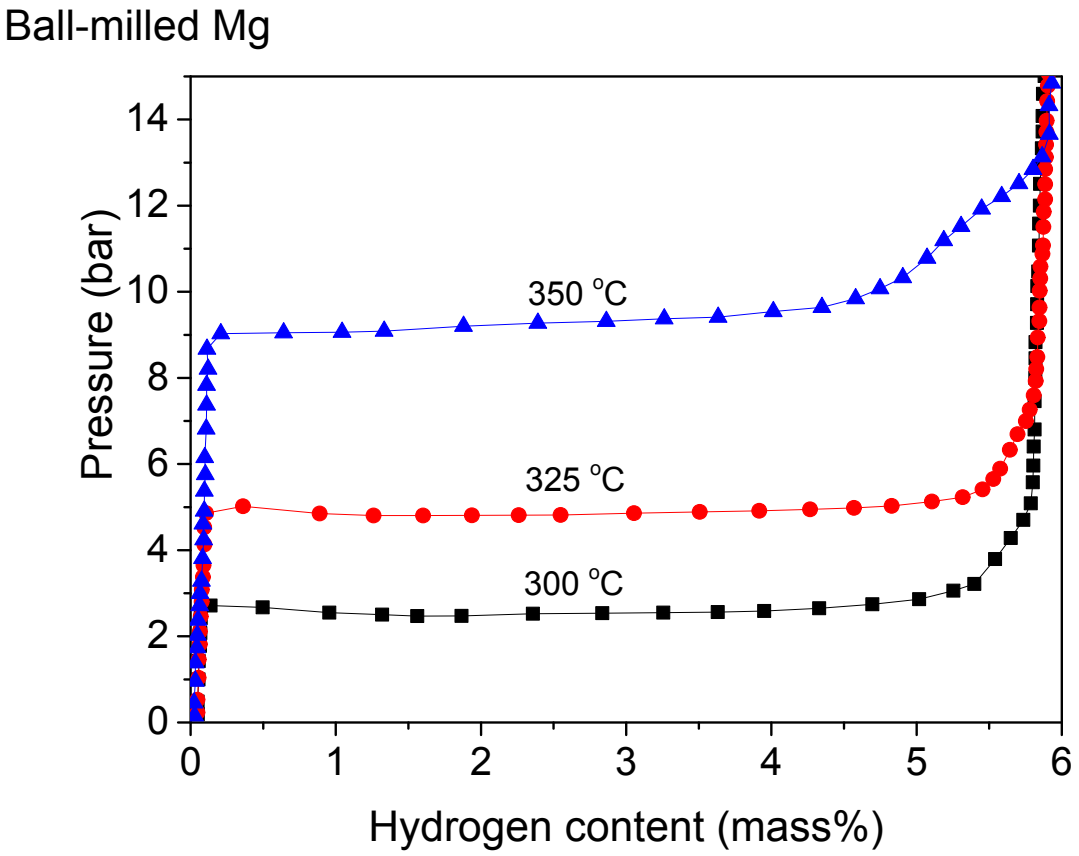

Fig. S12: PCI corresponding to the absorption of hydrogen with ball-milled MgH_2.

1. O. Friedrichs, J. C. Sanchez-Lopez, C. Lopez-Cartes, M. Dornheim, T. Klassen, R. Bormann and A. Fernandez, *Appl. Surf. Sci.*, 2006, **252**, 2334-2345.
2. E. Nasybulin, W. Xu, M. H. Engelhard, Z. Nie, S. D. Burton, L. Cosimbescu, M. E. Gross and J.-G. Zhang, *J. Phys. Chem. C*, 2013, **117**, 2635-2645.